TOXICOLOGICAL SCIENCES **118(2)**, 653–666 (2010)
doi:10.1093/toxsci/kfq272
Advance Access publication September 9, 2010

Adding Insult to Injury: Effects of Xenobiotic-Induced Preantral Ovotoxicity on Ovarian Development and Oocyte Fusibility

Alexander P. Sobinoff,* Victoria Pye,* Brett Nixon,*,† Shaun D. Roman,*,† and Eileen A. McLaughlin*,†,[1]

*Reproductive Science Group; and †Australian Research Council Center of Excellence in Biotechnology and Development, School of Environmental and Life Sciences, University of Newcastle, Callaghan, New South Wales 2308, Australia

[1]To whom correspondence should be addressed. Fax: +612-4921-6308. E-mail: eileen.mclaughlin@newcastle.edu.au.

Received July 7, 2010; accepted September 3, 2010

Mammalian females are born with a finite number of nonrenewing primordial follicles, the majority of which remain in a quiescent state for many years. Because of their nonrenewing nature, these "resting" oocytes are particularly vulnerable to xenobiotic insult, resulting in premature ovarian senescence and the formation of dysfunctional oocytes. In this study, we characterized the mechanisms of ovotoxicity for three ovotoxic agents, 4-vinylcyclohexene diepoxide (VCD), methoxychlor (MXC), and menadione (MEN), all of which target immature follicles. Microarray analysis of neonatal mouse ovaries exposed to these xenobiotics *in vitro* revealed a more than twofold significant difference in transcript expression ($p < 0.05$) for a number of genes associated with apoptotic cell death and primordial follicle activation. Histomorphological and immunohistological analysis supported the microarray data, showing signs of primordial follicle activation and preantral follicle atresia both *in vitro* and *in vivo*. Sperm-oocyte fusion assays on oocytes obtained from adult Swiss mice treated neonatally revealed severely reduced sperm-egg binding and fusion in a dose-dependent manner for all the xenobiotic treatments. Additionally, lipid peroxidation analysis on xenobiotic-cultured oocytes indicated a dose-dependent increase in oocyte lipid peroxidation for all three xenobiotics *in vitro*. Our results reveal a novel mechanism of preantral ovotoxicity involving the homeostatic recruitment of primordial follicles to maintain the pool of developing follicles destroyed by xenobiotic exposure and to our knowledge provide the first documented evidence of short-term, low- and high-dose (VCD 40–80 mg/kg/day, MXC 50–100 mg/kg/day, MEN 7.5–15 mg/kg/day) neonatal exposure to xenobiotics causing long-term reactive oxygen species–induced oocyte dysfunction.

Key Words: **xenobiotic; fertility; ovary; primordial follicle; oocyte dysfunction.**

The mammalian female reproductive life span is largely defined by a finite pool of primordial follicles established around the time of birth. These follicles serve as the primary source of all developing oocytes in the ovary and cannot be regenerated after fetal development (Hirshfield, 1991). Only a few primordial follicles are recruited into the growing pool of follicles at any one time, with some follicles remaining in a quiescent state for many years. This event occurs in regular waves and is continuous from birth until the primordial follicle pool is depleted, resulting in menopause (McGee and Hsueh, 2000). Overall, < 1% of all follicles recruited into the growing pool are destined for ovulation, with the vast majority being lost during development in an apoptotic process called atresia (Hirshfield, 1991). Although atresia is a normal physiological process, it is now known that it can be abnormally triggered through exposure to synthetic chemical compounds (or xenobiotics) with disastrous effects on female fertility (Hoyer and Sipes, 1996). Because of their nonrenewing nature, xenobiotics that destroy primordial follicles are particularly damaging to female fertility, causing permanent infertility and premature ovarian failure (Borgeest *et al.*, 2004; Borman *et al.*, 2000; Neal *et al.*, 2007).

Although the ovotoxic effects of many xenobiotics are well documented, the exact molecular mechanisms behind their action are only just being elucidated. One of the most extensively characterized mechanisms underpinning primordial follicle ovotoxicity has been explored using the xenobiotic 4-vinylcyclohexene diepoxide (VCD), an ovotoxic metabolite of 4-vinylcyclohexene used as a solvent for epoxides in industry (Hoyer and Sipes, 1996). Repeated dosing of VCD in rodents induces preantral follicle loss, specifically primordial and primary follicle destruction (Kao *et al.*, 1999). Molecular mechanistic studies demonstrate that VCD enhances follicular atresia in preantral follicles via the activation of Bcl-2 family of proto-oncogenes and proapoptotic members of the mitogen-activated protein kinase (MAPK) family (Hu *et al.*, 2001, 2002). VCD-induced primordial follicle ovotoxicity has also been shown to be nullified by phosphatidylinositol 3-kinase (PI3 kinase) inhibition *in vitro* (Keating *et al.*, 2009). As PI3 kinase is believed to be required for primordial follicle activation, growth, and survival, this suggests that VCD may induce primordial follicle loss through increased follicular activation (McLaughlin and McIver, 2009). Whereas increased follicle activation and atresia contributes to VCD-induced follicular atresia *in vitro*, the

entire *in vivo* mechanism underpinning VCD and other xenobiotic ovotoxicity remains unclear.

In addition to the molecular mechanisms behind xenobiotic ovotoxicity, the effects of xenobiotic exposure on long-term oocyte function have not been studied. One potential impact of xenobiotic exposure on egg and embryo quality is the induction of the formation of reactive oxygen species (ROS). Ovarian somatic and germ cells normally remove the harmful influence of xenobiotics through a three-tier enzymatic defence mechanism. The initial detoxification step involves the bioactivation of xenobiotic compounds into free radical intermediates by the cytochrome p450 family of oxidases (Danielson, 2002). Xenobiotic-enhanced ROS formation can occur in the oocyte via the unnatural uncoupling of the oxidative reaction or, if the hydroxylated metabolite forms a quinone, through redox cycling (Wells *et al*., 2009). In the mammalian ovary, cytochrome P450 enzyme mRNA levels rise in response to xenobiotic exposure (Cannady *et al*., 2003), potentially leading to disturbed oocyte redox potential, resulting in oxidative damage to cellular macromolecules and/or perturbed signal transduction (Tarin, 1996). In terms of oocyte functional competence, peroxidative damage to the oocyte plasma membrane lipids may also alter membrane fluidity and elasticity, inhibiting sperm/oocyte fusion and fertilization.

To better understand the mechanisms underpinning xenobiotic-induced ovotoxicity, we examined the effects of three ovotoxic environmental chemicals on ovarian follicle signaling pathways and oocyte dysfunction. In addition to VCD, the ovarian xenobiotics, methoxychlor (MXC), and menadione (MEN) were used in this study. MXC is a synthetic organochlorine insecticide that has been shown to directly induce follicular atresia *in vivo*, specifically targeting antral follicles in adult cycling female mice (Borgeest *et al*., 2004, 2002). Additionally, preliminary studies in our laboratory have also shown that MXC is capable of inducing primordial follicle loss in neonatal ovaries *in vitro*, possibly because of an independent mechanism of prepubertal ovotoxicity. The effects of the synthetic vitamin K quinone MEN on ovarian folliculogenesis have not been reported; however, pilot studies in our laboratory demonstrated that it is a potent ovotoxicant capable of inducing follicular atresia in neonatal ovaries cultured *in vitro*. Microarray, follicle counts, and immunohistological analysis revealed a consistent mechanism of primordial follicle activation in VCD and MXC ovotoxicity *in vitro* and all three xenobiotics *in vivo*. Sperm-oocyte fusion assays and lipid peroxidation analysis demonstrated that short-term xenobiotic exposure causes long-term oocyte dysfunction possibly because of xenobiotic ROS–induced oxidative stress.

MATERIALS AND METHODS

Reagents. Unless otherwise stated, chemicals, xenobiotics (> 95% purity), and custom-designed primers were purchased from Sigma Chemical Co. (St Louis, MO) and were of molecular biology or research grade. Mouse monoclonal anti-proliferating cell nuclear antigen antibody (anti-PCNA, NA03T) was obtained from Merck KGaA (Darmstadt, Germany). Rabbit polyclonal anti-active caspase 3 antibody (anti-Casp3, ab13847), rabbit polyclonal anti-active caspase 2 antibody (anti-Casp2, ab2251), mouse monoclonal anti-human p63 (anti-p63, ab3239), and rabbit polyclonal anti-cytochrome p450 2E1 (anti-Cyp2E1, ab73878) were obtained from Abcam (Cambridge, MA). Mouse monoclonal anti-8-oxoguanine (anti-8ox, MAB3560) was obtained from Chemicon (Billerica, MA). Alexa Fluor 594 goat anti-rabbit immunoglobulin G (IgG) (A11012), Alexa Fluor 594 goat anti-mouse IgG (A11005), 4,4-difluoro-5-(4-phenyl-1,3-buttadienyl)-4-bora-3a,4a-diaza-s-indacene-3-undecanoic acid 581/591 C11 (BODIPY; D3861), fetal bovine serum, L-glutamine, and Insulin-Transferrin-Selenium (ITS) were purchased from the Invitrogen Co. (Carlsbad, CA). L-Ascorbic Acid was obtained from MP Biomedicals (Solon, OH) and 0.4-μm Culture Plate Inserts were purchased from Millipore (Billerica, MA). All culture dishes and cell culture plates were obtained from Greiner Bio-One (Monroe, NC). Oligo(dT)15 primer, RNasin, dNTPs, M-MLV-Reverse Transcriptase, RQ1 DNAse, GoTaq Felxi, $MgCl_2$, GoTaq quantitative PCR (qPCR) master mix, and Proteinase K were purchased from the Promega Corporation (Madison, WI).

Animals. All experimental procedures involving the use of animals were performed with the approval of the University of Newcastle's Animal Care and Ethics Committee (ACEC). Inbred Swiss mice were obtained from a breeding colony held at the Institute's central animal facility and maintained according to the recommendations prescribed by the ACEC. Mice were housed under a controlled lighting regime (16L:8D) at 21–22°C and supplied with food and water *ad libitum*.

Animal dosing. Female Swiss neonatal mice (day 4, 6–10 animals per treatment group) were weighed and administered (ip) 7 daily, consecutive doses of either sesame oil containing vehicle control (< 0.5 ml/kg/day dimethyl sulfoxide [DMSO]) or sesame oil containing a low and high dose of VCD (40 and 80 mg/kg/day), MXC (50 and 100 mg/kg/day), or MEN (7.5 and 15 mg/kg/day). The dosage, routes of administration, and dosing time courses were based on previous studies and were chosen with the intention of inducing partial ovotoxicity with minimal cytotoxicity (Borgeest *et al*., 2002; Cannady *et al*., 2003; Gupta *et al*., 2006; Radjendirane *et al*., 1998). Animals were observed daily for symptoms of toxicity and mortality. Half of the treated animals were culled by CO_2 asphyxiation 24 h after the last injection. The remaining animals were weaned and then superovulated at 6 weeks of age via ip injection of 10 IU of Folligon (equine chorionic gonadotropin; Intervet, Sydney, Australia) followed by ip administration of 10 IU of Chorulon (human chorionic gonadotrophin [hCG]; Intervet) 48 h later.

Ovarian culture. Ovaries from days 3–4 Swiss neonatal mice were cultured as described previously (Holt *et al*., 2006). Briefly, Swiss neonates were sacrificed by CO_2 inhalation followed by decapitation. Ovaries were excised, trimmed of excess tissue, and placed on culture plate inserts in six-well tissue culture plate wells floating atop 1.5 ml Dulbecco's Modified Eagle Medium: Nutrient Mixture F-12 medium containing 5% (vol/vol) fetal calf serum, 1 mg/ml bovine serum albumin (BSA), 50 μg/ml ascorbic acid, 27.5 μg/ml ITS, 2.5mM glutamine, and 5 U/ml penicillin/streptomycin. Media were supplemented with 40 ng/ml basic fibroblast growth factor, 50 ng/ml leukemia inhibitory factor, and 25 ng/ml stem cell factor. Using fine forceps, a drop of medium was placed over the top of each ovary to prevent drying. Ovaries were cultured for 4 days at 37°C and 5% CO_2 in air, with media changes every 2 days. Ovaries were treated with vehicle control medium (0.1% DMSO), VCD (25μM), MXC (25μM), or MEN (5μM). Xenobiotic culture concentrations were determined by pilot studies performed in our laboratory with the intention of inducing overt toxicity.

Histological evaluation of follicles. Following *in vitro* culture/*in vivo* dosing, ovaries were placed in Bouin's fixative for 4 h, washed in 70% ethanol, paraffin embedded, and serially sectioned (4 μm thick) throughout the entire ovary, with every fourth slide counterstained with hematoxylin and eosin.

Healthy oocyte–containing follicles were then counted in every hematoxylin- and eosin-stained section. Follicles with eosinophilic oocytes were not counted as they could not be definitively identified as follicles. Primordial follicles were classified as those with a single layer of squamous granulosa cells. Activating follicles were identified as those that contained one or more cuboidal granulosa cells in a single layer. Primary follicles were classified as those that contained more than four cuboidal granulosa cells in a single layer. Secondary follicles were identified as those with two layers of granulosa cells, and preantral follicles were classified as those with more than two layers of granulosa cells. Both *in vitro*– and *in vivo*–treated ovaries did not contain follicles beyond the preantral stage.

Immunohistochemistry. Ovaries for immunohistochemistry were fixed in Bouin's and sectioned 4 μm thick. PCNA, active Casp2 and active Casp3 were stained using the same protocol with the exception of the primary antibody. Slides were deparaffinized in xylene and rehydrated with subsequent washes in ethanol. Antigen retrieval was carried out by microwaving sections for 3 × 3 min in Tris buffer (50mM, pH 10.6). Sections were then blocked in 3% BSA/tris-buffered saline (TBS) for 1.5 h at room temperature. The following solutions were diluted in TBS containing 1% BSA. Sections were incubated with anti-PCNA (1:80), anti-Casp2 (1:200), or anti-Casp3 (1:200) for 1 h at room temperature. After washing in TBS containing 0.1% Triton X-100, sections were incubated with the appropriate fluorescent-conjugated secondary antibodies (Alexa Fluor 594 goat anti-rabbit IgG and Alexa Fluor 594 goat anti-mouse IgG; 1:200 dilution) for 1 h. Slides were then counterstained with 4′-6-diamidino-2-phenylindole (DAPI) for 5 min, mounted in Mowiol, and observed on an Axio Imager A1 fluorescent microscope (Carl Zeiss MicroImaging, Inc., Thornwood, NY) under fluorescent optics and pictures taken using an Olympus DP70 microscope camera (Olympus America, Center Valley, PA).

TUNEL analysis. Bouin's fixed sections were deparaffinized and rehydrated as mentioned previously. Sections were then boiled in Tris buffer (50mM, pH 10.6) for 20 min and treated with 20 μg/ml Proteinase K for 15 min in a humidified chamber. Terminal deoxynucleotidyl transferase dUTP nick end labeling (TUNEL) analysis was then performed using an In Situ Cell Death Detection Kit, Fluorescein (Roche Diagnostics Pty Ltd.; Dee Why, New South Wales, Australia), according to the manufacturer's instructions. Slides were then counterstained with DAPI for 5 min, mounted in Mowiol, and observed on an Axio Imager A1 fluorescent microscope (Carl Zeiss) under fluorescent optics and pictures taken using an Olympus DP70 microscope camera (Olympus).

Protein extraction and immunoblotting. Ovaries were solubilized with SDS lysis buffer and quantified aliquots separated by electrophoresis and transferred onto a nitrocellulose Hybond C-Extra membrane (Amersham) prior to blocking for 2 h in 5% skim milk powder in TBST (0.1% Tween-20) and then incubated in a 1:1000 dilution of anti-Cyp2E1 in 1% BSA/TBST overnight at 4°C. Following washing and incubation with horseradish peroxidase-conjugated goat anti-rabbit secondary antibody (Santa Cruz, sc-2004) at a 1:5000 dilution for 1 h at room temperature, proteins were visualized using an ECL Detection Kit (Amersham) according to manufacturer's instructions. The membrane was then stripped in 100mM β-mercaptoethanol, 2% SDS, and 62.5mM Tris (pH 6.7) at 60°C for 1 h and reprobed using a mouse monoclonal anti-α-tubulin (Sigma, T5168) as a loading control.

RNA extraction. Total RNA was isolated from ovaries using two rounds of a modified acid guanidinium thiocyanate-phenol-chloroform protocol (Chomczynski and Sacchi, 1987): washed cells resuspended in lysis buffer (4M guanidinium thiocyanate, 25mM sodium citrate, 0.5% sarkosyl, 0.72% β-mercaptoethanol). RNA was isolated by phenol/chloroform extraction and isopropanol precipitated.

Real-time PCR. Reverse transcription was performed with 2 μg of isolated RNA, 500 ng oligo(dT)15 primer, 40 U of RNasin, 0.5mM dNTPs, and 20 U of M-MLV-Reverse Transcriptase. Total RNA was DNase treated prior to reverse transcription to remove genomic DNA. Real-time PCR was performed using SYBR Green GoTaq qPCR master mix according to manufacturer's instructions on an MJ Opticon 2 (MJ Research, Reno, NV). Primer sequences along with annealing temperatures have been supplied as supplementary data (Supplementary table 3). Reactions were performed on cDNA equivalent to 100 ng of total RNA and carried out for 40 amplification cycles. SYBR Green fluorescence was measured after the extension step at the end of each amplification cycle and quantified using Opticon Monitor Analysis software Version 2.02 (MJ Research). For each sample, a replicate omitting the reverse transcription step was undertaken as a negative control. Reverse transcription reactions were verified by β-actin PCR performed for each sample in all reactions in triplicate. Real-time data were analyzed using the equation $2^{-\Delta\Delta C(t)}$, where $C(t)$ is the cycle at which fluorescence was first detected above background fluorescence. Data were normalized to "cyclophilin," "beta-2-microglobulin," and "beta-glucuronidase" and are presented as the average of each replicate normalized to an average of the reference genes (± SEM).

Microarray analysis. Total RNA (approximately 5 μg) was isolated from xenobiotic-cultured neonatal ovaries and prepared for microarray analysis at the Australian Genome Research Facility (AGRF) using an Affymetrix Mouse Genome 430 2.0 Array platform. Labeling, hybridizing, washing, and array scanning were performed by the AGRF using the Affymetrix protocol on a GeneChip scanner 3000 (Affymetrix, Santa Clara, CA). All experiments were performed in triplicate with independently extracted RNAs. Data analysis and normalization were also performed by AGRF using the Robust Multichip Average method. Briefly, control (DMSO)-treated neonatal ovaries were used as a background to generate expression signal log ratios with basis 2 to determine fold changes (*n*-fold) between control- and xenobiotic-treated ovaries. Statistically significant genes with more than a twofold difference in gene expression determined through the use of a "volcano plot" were then analyzed using Ingenuity Pathways Analysis (IPA) (Ingenuity Systems, Redwood City, CA) software to identify canonical signaling pathways influenced by xenobiotic exposure. The data discussed in this publication have been deposited in National Center for Biotechnology Information's Gene Expression Omnibus (GEO) and are accessible through GEO Series accession number GSE23725 (http://www.ncbi.nlm.nih.gov/geo/query/acc.cgi?acc=GSE23725).

Sperm-oocyte fusion assay. Adult mice (6 weeks) treated with xenobiotics over a 7-day period after birth were superovulated as described previously under animal dosing. Cumulus-intact oocytes were recovered 12–15 h after the final hCG injection by rupturing the oviductal ampullae of superovulated animals in M2 medium. Adherent cumulus cells were then dispersed by treating the collected oocytes with 300 IU/ml hyaluronidase solution and washing twice in M2 medium under oil. The zona pellucida was then removed from these oocytes by brief treatment with low-pH (2.5) acid Tyrode's solution and allowed to recover for at least 1 h at 37°C in an atmosphere of 5% CO_2 in air. Sperm were collected from mature male mice by dissecting the cauda epididymides and squeezing out the dense sperm mass along the tube. The sperm were then allowed to disperse into 800 μl M2 medium, diluted to a final concentration of 2×10^5 sperm per milliliter in M2 medium, and allowed to capacitate for 3 h at 37°C in 5% CO_2 in air. Following capacitation, zona-free oocytes were preloaded with DAPI for 15 min; 12–25 oocytes were then added to the sperm suspensions and coincubated for 15 min at 37°C in 5% CO_2 in air. Using serial aspiration through a finely drawn pipette, unbound and loosely adhered spermatozoa were removed from oocytes. Oocytes were then mounted on slides and the number of sperm bound to the oocyte membrane counted using phase contrast microscopy. Sperm-oocyte fusion was then assayed by counting the number of DAPI-stained sperm heads attached to the oocyte membrane using fluorescent microscopy.

Oocyte lipid peroxidation assay. Adult female mice (6–8 weeks) were superovulated, oocytes recovered, and adherent cumulus cells removed as described previously. Oocytes were then treated with vehicle control medium (0.1% DMSO) or xenobiotics (5, 15, and 25μM) for 2 h under oil at 37°C and 5% CO_2 in air. An oxidative stress–positive control was also carried out by exposing oocytes to 80mM H_2O_2 for 30 min under oil at 37°C and 5% CO_2 in air. Oocytes were then washed twice in M2 medium under oil and incubated in 10mM BODIPY stain for 30 min at 37°C in 5% CO_2 in air. The dye-loaded oocytes were then washed twice in M2 medium and mounted on slides. Green and red

fluorescence of BODIPY were determined using an LSM510 laser-scanning microscope (Carl Zeiss MicroImaging, Inc.) equipped with argon and helium/neon lasers at excitation wavelengths of 488 and 543 nm and emission spectra of 500–530 nm (green) and greater than 560 nm (red). Histogram analysis was then used to determine the ratio of green to red fluorescence.

Statistics. Comparisons between the control and treatment groups were performed using one-way ANOVA and Tukey's Honestly Significant Difference test. The assigned level of significance for all tests was $p < 0.05$.

Experimental design. A summary of the experimental design can be found in supplementary data (Supplementary fig. 1).

RESULTS

Influence of Xenobiotic Exposure on the Neonatal Ovary Transcriptome

All three xenobiotic treatments led to significant differences in ovarian gene expression (Fig. 1). Similarities between the neonatal ovarian responses to all three xenobiotics were assessed using Ingenuity Pathways comparison analysis software (IPA) (Fig. 1D; Supplementary table 1). Overall, only six genes were commonly regulated between the three xenobiotic-treated groups. However, 70 common genes were regulated in response to VCD and MXC exposure, making up 6% of the total number of genes affected by VCD and 16% of the total number of genes affected by MXC. This suggested an overlapping mechanism between VCD- and MXC-induced ovotoxicity.

Significantly altered genes were then categorized according to biological function (Table 1). In agreement with the current literature, xenobiotic exposure influenced a large number of genes involved in cell death. Interestingly, all three xenobiotics also influenced the expression of genes implicated in the cell cycle, cellular assembly and organization, development, and growth/proliferation. This indicated that the observed ovarian follicular response to these xenobiotics was not limited to follicular atresia but also involved a number of other biological processes.

VCD and MXC Exposure Upregulate Signaling Pathways Implicated in Follicular Development and Atresia

In order to confirm a multilayered mechanism of xenobiotic-induced preantral ovotoxicity involving various biological functions in neonatal ovaries, differentially expressed genes were analyzed for signaling pathways and molecular functions using IPA (Fig. 2; Supplementary Table 2). VCD exposure caused the significant upregulation of a large number of canonical signaling pathways associated with follicular development (vascular endothelial growth factor [VEGF], peroxisome proliferator-activated receptor alpha/retinoid X receptor alpha, Integrin, and insulin-like growth factor 1 signaling) and primordial follicle activation (Phosphatidylinositol 3-kinase/serine-threonine protein kinase [PI3K/Akt], mammalian target of rapamycin, and extracellular signal-regulated kinase/MAPK signaling) in contrast to a small number of pathways involved in follicular atresia (PTEN, protein 53 [p53], and myelocytomatosis oncogene (myc)-mediated apoptosis signaling). MXC exposure also resulted in

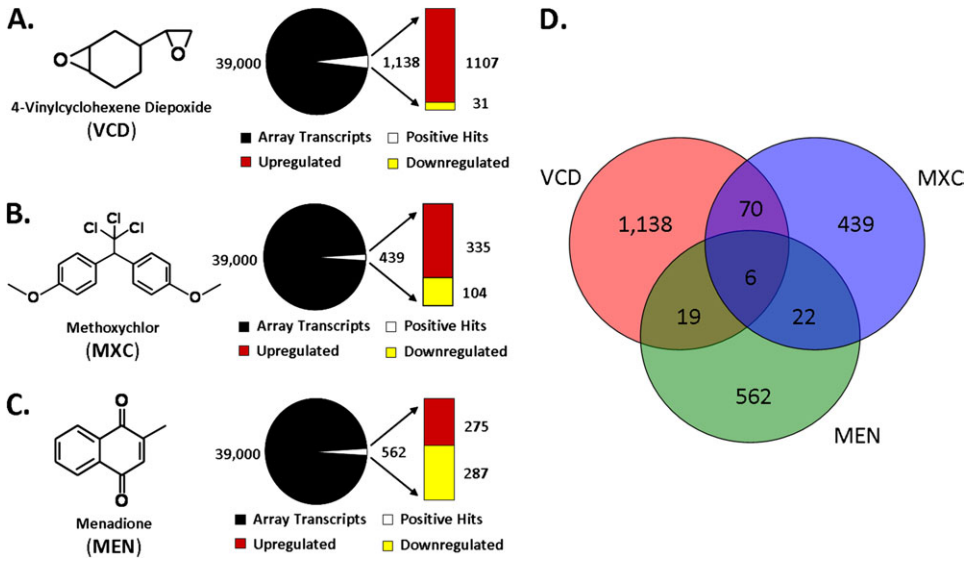

FIG. 1. Microarray analysis of DMSO-cultured ovaries versus xenobiotic-cultured ovaries. Ovaries were excised from neonatal mice (4 days old, $n = 15$) and cultured in xenobiotic-treated medium for 96 h, RNA extracted, and prepared for microarray analysis as described in the Materials and Methods section. (A–C) Summary of microarray results for each xenobiotic treatment. Total number of genes found on an Affymetrix Mouse Genome 430 2.0 Array platform are presented as nonregulated (black) and regulated (white) genes with a significant change in expression (> twofold change, $p < 0.05$). The top bar represents the number of positively regulated genes, and the bottom bar represents the number of negatively regulated genes in xenobiotic-cultured ovaries. (D) Venn diagrams of genes with significantly altered gene expression in xenobiotic-cultured ovaries. Between the VCD- and MXC-cultured ovaries, 70 common genes were regulated in response to xenobiotic exposure.

TABLE 1

Functional Classification of Genes that Were Upregulated or Downregulated by Xenobiotic Exposure in Cultured Neonatal Ovaries. Genes Were Analyzed Using IPA (Ingenuity Systems) for Molecular and Cellular Functions. Only Those Genes Exhibiting a Greater than Twofold Change in Expression Were Categorized ($p < 0.05$). Note that Some Genes Are Listed in Multiple Functional Groups

	VCD		MXC		MEN	
Molecular and cellular function	Upregulated	Downregulated	Upregulated	Downregulated	Upregulated	Downregulated
Cell cycle	50	1	21	2	2	4
Cell death	129	4	33	12	20	19
Cell morphology	65	2	31	5	14	14
Cell signaling	5	1	11	5	12	5
Cell-to-cell signaling and interaction	40	—	18	11	27	15
Cellular assembly and organization	64	1	38	4	17	13
Cellular development	151	4	50	16	18	33
Cellular function and maintenance	43	3	28	6	19	14
Cellular growth and proliferation	129	4	13	18	12	25
DNA replication and repair	24	1	12	6	3	13
Gene expression	102	2	38	4	3	21

the significant upregulation of canonical signaling pathways associated with follicular development (retinoic acid receptor activation, VEGF, granulocyte-macrophage colony stimulating factor, Gα12/13, and aryl hydrocarbon receptor signaling), primordial follicle activation (PI3K/Akt signaling), and follicular atresia (PTEN, p53, myc-mediated apoptosis, and apoptosis signaling). However, unlike VCD and MXC, MEN only influenced two pathways implicated in follicular atresia (ataxia telangiectasia–mutated gene and β-alanine signaling) and a number of other pathways involved in the immune response and xenobiotic metabolism.

qPCR Validation of Microarray Results: VCD and MXC Upregulate Common Genes Involved in Folliculogenesis

Validation of the microarray results using qPCR confirmed the upregulation of all 10 selected genes in both VCD- and MXC-cultured ovaries (Table 2). Of these genes, two (*MAPK8* and *Bcl2l1*) had been associated with either VCD- or MXC-induced atresia, *Ccnd2* has been implicated in MXC ovotoxicity, and two were linked with the PTEN/PI3K/PDK1/Akt signaling pathway, which has been coupled with VCD-induced primordial follicle activation (*Akt1* and *Akt2*). The remaining five genes were novel and two have been implicated in apoptosis (*Med1* and *Cdkn2a*) and the other three in later follicular development (*Sox4*, *Dlg4* and *Ccnd2*). These results suggest that MXC and VCD have additional ovotoxicity mechanisms.

Effects of Xenobiotic Exposure on Primordial Follicle Activation and Follicular Atresia In Vitro

Neonatal ovaries cocultured with xenobiotics were probed for markers of primordial follicle activation and cell death. PCNA staining was detected in the granulosa cells and oocyte nuclei of primary and secondary follicles in vehicle control (DMSO)–cultured ovaries and was absent in primordial follicles, indicating that they were in their quiescent state (Fig. 3). However, PCNA staining was detected in both the granulosa cells and the oocytes of primordial follicles in all three xenobiotic-cultured ovaries, indicating a commitment to follicular development. In contrast to the vehicle control, both active Casp2 and Casp3 were detected in the majority of primary and secondary follicles in all three xenobiotic-cultured ovaries, with active Casp2 being localized to developing oocytes and active Casp3 to developing granulosa cells (Fig. 3). Interestingly, both activated Casp2 and Casp3 were not detected in any primordial follicles in the xenobiotic-cultured ovaries. This suggests that both the granulosa cells and the oocytes of developing preantral follicles had committed to apoptosis, but not primordial follicles. TUNEL staining was also detected in primary and secondary stage follicles in both VCD- and MXC-cultured ovaries but was detected in all follicle types in MEN-treated ovaries, indicating widespread DNA damage. These results indicate selective apoptosis in developing preantral follicles in both VCD- and MXC-cultured ovaries and widespread cell death in MEN-cultured ovaries.

Effects of Xenobiotic Exposure on Primordial Follicle Activation and Follicular Atresia In Vivo

Female Swiss neonatal mice were administered daily injections of either high- or low-dose xenobiotic for 7 days. PCNA was detected in large clusters of primordial follicles in all three high-dose xenobiotic treatments (Fig. 4), with a staining pattern similar to that observed *in vitro*. The follicular composition of ovaries from all three low-dose xenobiotic treatments revealed an observable reduction in the number of preantral follicles (Fig. 5A). The low-dose VCD treatment also induced a slight but significant reduction in the

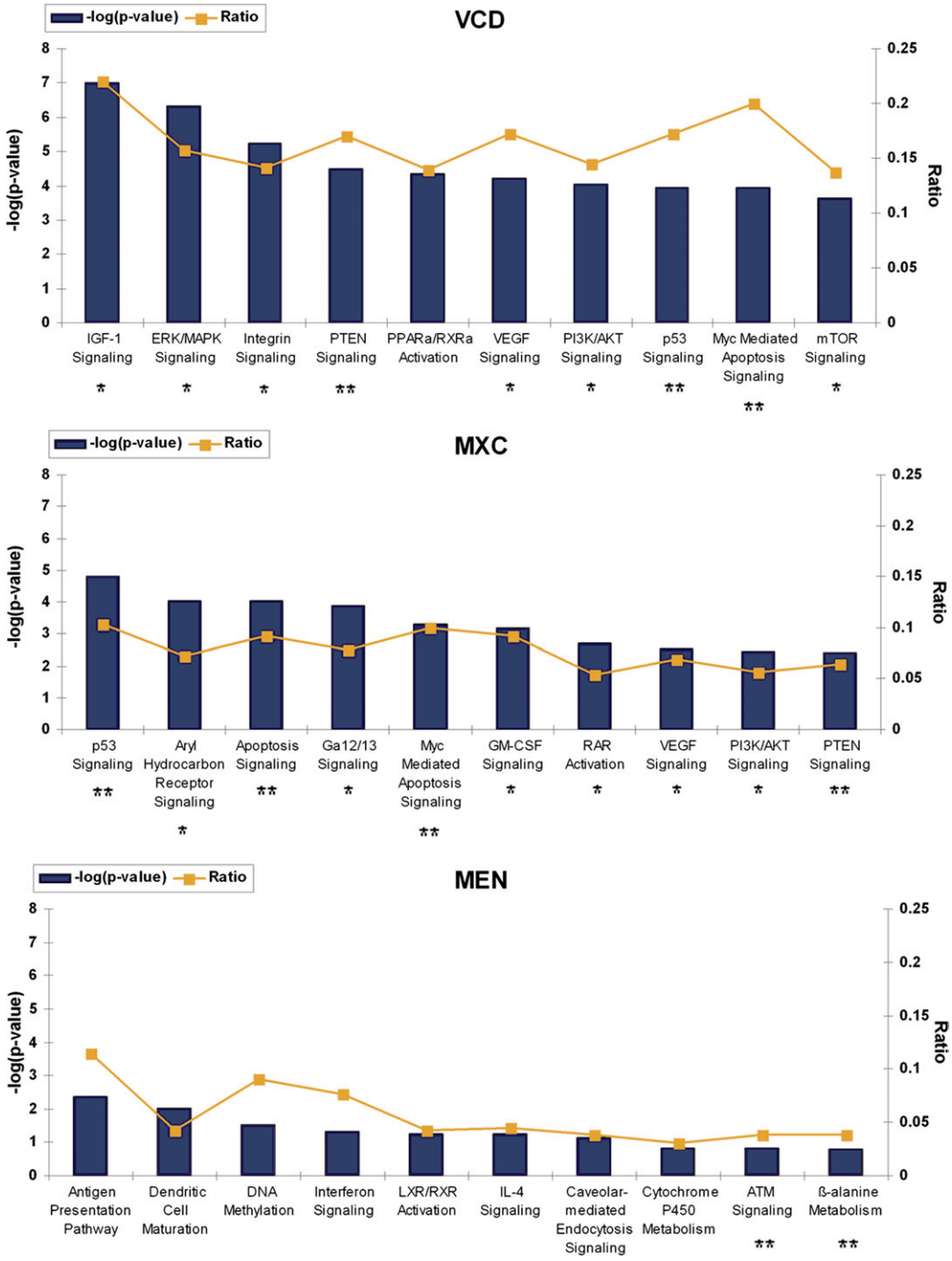

FIG. 2. Top canonical pathways that were significantly upregulated by xenobiotic-cultured neonatal ovaries as identified by IPA. The significance of the association between upregulated genes and the canonical pathway was evaluated using a right-tailed Fisher's exact test to calculate a *p* value determining the probability that the association is explained by chance alone (y-axis). Ratios referring to the proportion of upregulated genes from a pathway related to the total number of molecules that make up that particular pathway are also displayed (line graph, z-axis). Asterisks indicate pathways associated with follicular development, and double asterisks indicate pathways associated with follicular atresia.

number of primordial follicles, mirrored by a comparable increase in activating primordial follicles. Both the low-dose MXC and MEN treated ovaries also revealed a slight reduction in the number of secondary follicles, although this was not significant. Analysis indicated that the low-dose MEN treatment induced a significant decrease in follicular number (54% of the control). In agreement with the PCNA results, the follicular composition of ovaries from all three high-dose

TABLE 2

qPCR Validation of Microarray Results for Select Transcripts Upregulated by VCD- and MXC-Cultured Neonatal Ovaries. Total RNA Was Isolated from Xenobiotic-Cultured Ovaries, Reverse Transcribed, and qPCR Performed with Primers Specific for the cDNA of Indicated Genes as Described in the Materials and Methods section. Fold Change (Mean ± SE) and Summary of Function Relating to Folliculogenesis Are Included. All Fold Changes Were Statistically Significant ($p < 0.05$)

Gene symbol	Gene name	Summary of function	Fold change	
			VCD	MXC
Sox4	SRY-box–containing gene 4	Transcription factor; positive regulator of the Wnt receptor pathway implicated in folliculogenesis (Sinner *et al*., 2007)	5.34 ± 0.9	6.34 ± 0.5
Akt1	Thymoma viral proto-oncogene 1	Member of the PTEN/PI3K/PDK1/Akt signaling pathway implicated in follicle activation and granulosa cell proliferation (Brown *et al*., 2010; Reddy *et al*., 2009)	4.58 ± 0.4	4.54 ± 0.4
Akt2	Thymoma viral proto-oncogene 2	Implicated in primordial germ cell growth, cell death, and proliferation (Brown *et al*., 2010; Datta *et al*., 1999)	2.72 ± 0.2	1.73 ± 0.1
Dlg4	Discs, large homolog 4 (Drosophila)	Plasma membrane kinase; expressed in activated primordial follicle granulosa cells with a suspected role in regulating folliculogenesis (Huang *et al*., 2003)	2.85 ± 0.5	2.17 ± 0.3
Ccnd2	Cyclin D2	Essential for granulosa cell proliferation, decreased expression associated with MXC antral follicle ovotoxicity (Gupta *et al*., 2006; Muñiz *et al*., 2006)	4.25 ± 0.7	4.26 ± 0.5
Mapk8	Mitogen-activated protein kinase 8	Increased expression is associated with VCD-induced atresia (Hu *et al*., 2002)	2.02 ± 0.3	4.81 ± 1.3
Bcl2l1	Bcl-2-like 1	Associated with granulosa cell proliferation and survival; overexpression reduces MXC ovotoxic effect in antral follicles (Borgeest *et al*., 2004; Brown *et al*., 2010; Rucker *et al*., 2000)	3.22 ± 0.3	2.98 ± 0.7
Rarg	Retinoic acid receptor, gamma	Expressed in primary follicle granulosa cells; shown to transcriptionally inhibit FSH receptor transcription (Kascheike and Walther, 1997; Xing and Sairam, 2002)	2.40 ± 0.1	1.71 ± 0.1
Cdkn2a	Cyclin-dependent kinase inhibitor 2A	Increased expression associated with follicular atresia; decreased expression associated with primordial follicle activation (Bayrak and Oktay, 2003)	4.92 ± 0.6	2.89 ± 0.2
Med1	Mediator complex subunit 1	DNA repair gene involved in p53-dependent apoptosis (Frade *et al*., 2002)	2.99 ± 0.3	2.80 ± 0.2

Note. SRY, sex-determining region Y; Wnt, wingless; FSH, follicle-stimulating hormone.

xenobiotic treatments indicated a large significant reduction in primordial follicles, with a comparably large increase in the number of activating follicles (Fig. 5B). Additionally, the high-dose xenobiotic treatments also caused a similar decrease in the number of preantral follicles to that observed in the low-dose treatments. Individually, VCD caused no further changes in follicular composition, MXC caused a significant increase in the composition of primary (~fourfold increase) and secondary (~twofold increase) follicles, and MEN caused an observable increase in the composition of primary follicles (~twofold increase). Analysis of the average number of follicles per section demonstrated a significant decrease in follicular number for VCD (43% of the control), MXC (59% of the control), and MEN (53% of the control).

Short-Term Xenobiotic Exposure Reduces Long-Term Oocyte Fusibility In Vivo

Adult Swiss mice treated with either a low or a high dose of xenobiotics for a 7-day period after birth were superovulated and their oocytes tested in sperm-oocyte fusion assays. Oocytes from both low- and high-dose xenobiotic treatments exhibited severely reduced sperm-egg binding compared with the control, with both MXC and MEN oocytes exhibiting a dose-dependent response (Fig. 6B). Similarly, sperm-egg fusion was

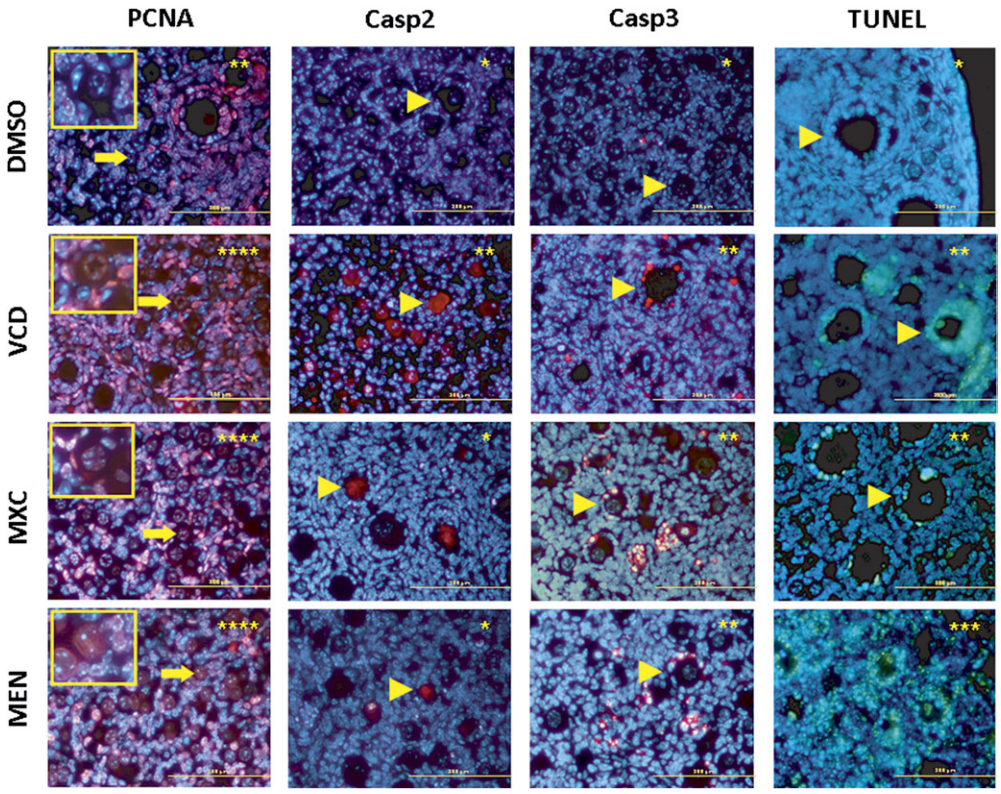

FIG. 3. Fluorescent immunohistological and TUNEL staining as visualized via fluorescent microscopy. Ovaries excised from neonatal mice (4 days old) were cultured in xenobiotic-treated medium for 96 h and processed for immunohistochemistry and TUNEL analysis as described in the Materials and Methods section. Ovarian sections were incubated with antibodies against PCNA, active caspase 2, and active caspase 3 or subjected to TUNEL analysis. The results presented here are representative of $n = 3$ experiments. The percentage of labeled follicles per section is represented by the following scale: * = < 25%, ** = 25–50%, *** = 51–75%, and **** = 76–100%. Thin arrow, primordial follicle; arrow head, primary follicle; scale bar is equal to 100 μm.

reduced to ~20% of the control for all three low-dose xenobiotic treatments, with negligible levels of sperm-egg fusion being detected in the oocytes from high-dose exposure (Fig. 6C). These results are intriguing, as they indicate that neonatal exposure to low doses of xenobiotic, which do not cause drastic changes in follicular composition (see Fig. 5A), will significantly reduce oocyte function.

Xenobiotic Exposure Induces Oocyte Lipid Peroxidation In Vitro

To investigate the possibility of xenobiotic-induced oocyte dysfunction resulting from peroxidative damage to the oocyte plasma membrane, lipid peroxidation studies using the fluorescent dye BODIPY were performed on ovulated MII oocytes exposed to xenobiotics *in vitro*. BODIPY is a fluorescent fatty acid analog, which shifts its emission peak from 560 (red) to 500–530 nm (green) upon the oxidation of fatty acids. In these experiments, MXC was substituted for its more ovotoxic metabolite 2,2-bis-(*p*-hydroxyphenyl)-1,1,1-trichloroethane, as MXC itself had no effect on lipid peroxidation (data not shown). All three xenobiotic treatments were capable of significantly inducing varying levels of lipid peroxidation *in vitro* (Fig. 7), and these results confirm the possibility of decreased sperm-egg binding/fusion observed *in vivo* being partially because of peroxidative damage to the oocyte plasma membrane.

DISCUSSION

Microarray analysis indicated a multilayered mechanism of xenobiotic-induced preantral ovotoxicity for both VCD and MEN involving follicular growth/development and atresia. Previous studies have also implicated increased follicular growth/development in VCD-induced ovotoxicity through PI3 kinase–dependent primordial follicle depletion in rodents (Hu *et al.*, 2006; Keating *et al.*, 2009). Indeed, in our study, VCD also upregulated the expression of genes involved in the PI3K/Akt signaling pathway, providing further support for this pathway in VCD-induced ovotoxicity. However, MXC has only been implicated in antral follicle atresia in adult rodents (Borgeest *et al.*, 2002, 2004) and the inhibition of antral follicle growth (Gupta *et al.*, 2009). Those experiments using adult cycling rodents are at odds with our unique findings of MXC upregulating pathways associated with follicular growth/development in neonatal ovaries. This difference may be because

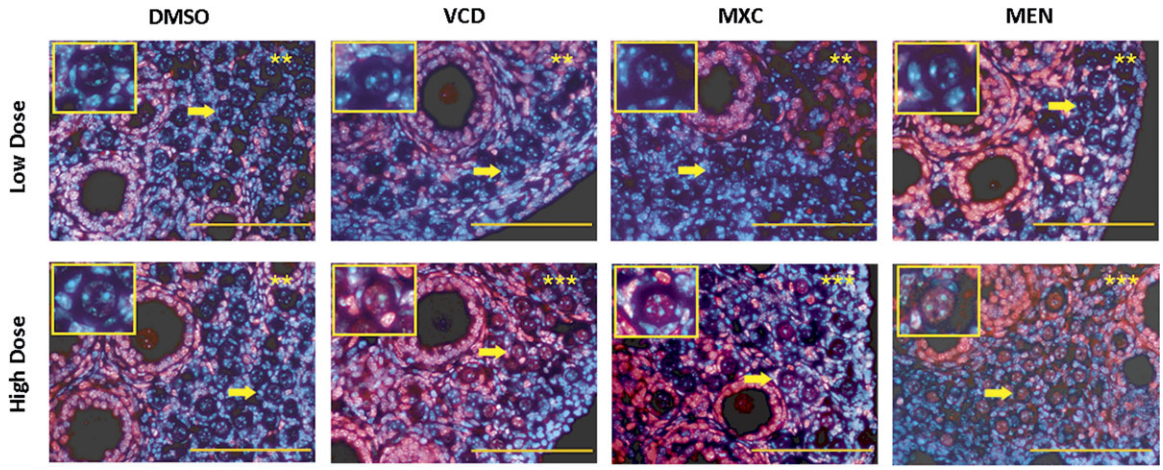

FIG. 4. Fluorescent immunolocalization of PCNA protein in low and high dose xenobiotic–treated ovaries *in vivo*. Neonatal mice (4 days old) were treated with either a low or a high dose of xenobiotics over a 7-day period, culled, and their ovaries extracted and processed for immunohistochemistry as outlined in the Materials and Methods section. The results presented here are representative of $n = 3$ experiments. The percentage of labeled follicles per section is represented by the following scale: * = < 10%, ** = 10–50%, *** = 51–75%, and **** = 76–100%. Thin arrow, primordial follicle; scale bar is equal to 100 μm.

of an independent mechanism of MXC-induced prepubertal ovotoxicity, as evidenced by age-dependent differences between the disposition and metabolism of xenobiotics.

In addition to the global similarities between VCD and MXC upregulated signaling pathways implicated in follicular growth/development and atresia, both xenobiotics influenced a number of common signaling pathways, suggesting an overlapping mechanism of ovotoxicity (Fig. 2). In further support of this hypothesis, qPCR analysis confirmed the upregulation of 10 genes in VCD- and MXC-cultured ovaries, five of which have not been previously associated with preantral ovotoxicity (Table 2). Two isoforms belonging to the Akt family of serine/threonine-directed kinases, *Akt1* and *Akt2*, were found to be upregulated by VCD and MXC. Both kinases have been

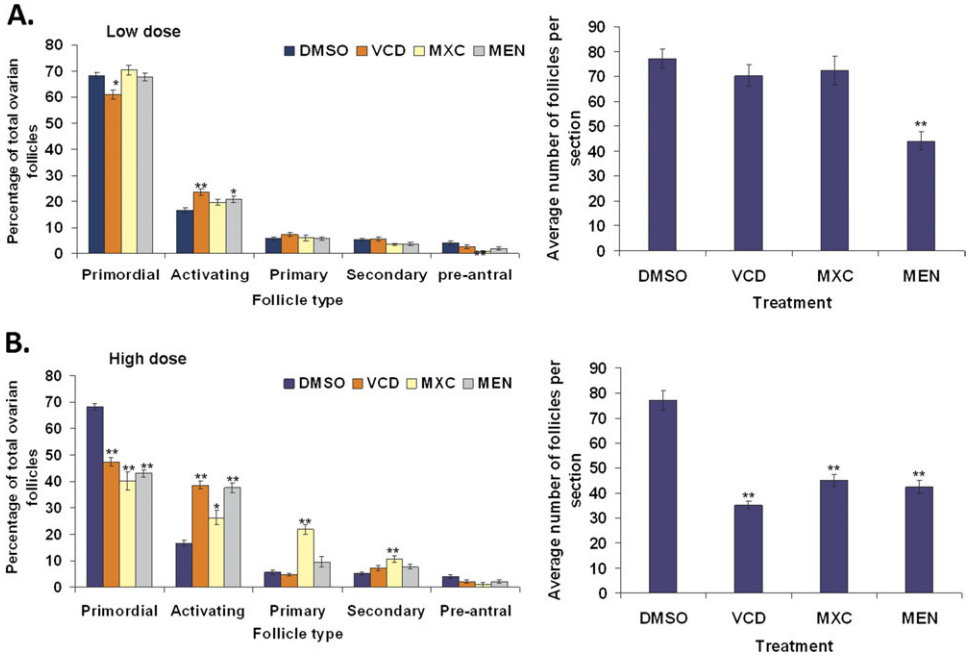

FIG. 5. Effect of xenobiotic exposure on ovarian follicle composition and number *in vivo*. Neonatal mice (4 days old) were treated with either a low or a high dose of xenobiotics over a 7-day period as described in the Materials and Methods section. Ovarian sections were stained with hematoxylin and eosin, and healthy oocyte–containing follicles were classified and counted under a microscope. (A) Low-dose ovarian follicle composition (left panel) and average number of follicles per counted section (right panel). (B) High-dose ovarian follicle composition (left panel) and average number of follicles per counted section (right panel). Values are mean ± SEM, $n = 3$–5 ovaries from three to five mice. The symbols * and ** represent $p < 0.05$ and $p < 0.01$, respectively, in comparison with DMSO control values.

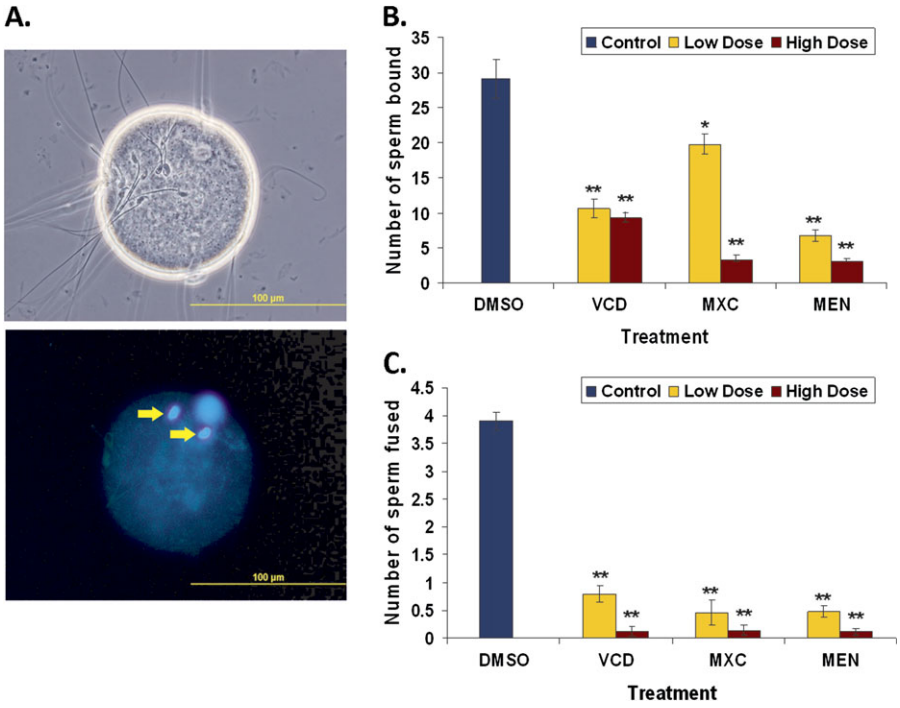

FIG. 6. Effect of neonatal xenobiotic exposure on long-term oocyte quality *in vivo*. Neonatal mice (4 days old) were treated with either a low or a high dose of xenobiotics over a 7-day period, weaned, and superovulated at 6 weeks of age. Collected zona-free oocytes were then coincubated with sperm and assessed for impaired sperm-egg binding and fusion as outlined in the Materials and Methods section. (A) Corresponding phase contrast and fluorescent microscopy images of control zona-free oocyte after sperm-egg binding assay. Arrows, fused sperm nuclei. Scale bar is equal to 100 µm. (B) Number of sperm heads bound to zona-free oocytes after coincubation. (C) Number of fused sperm observed after coincubation. Values are mean ± SE, $n = 12–25$ oocytes from three mice. The symbols * and ** represent $p < 0.05$ and $p < 0.01$, respectively, in comparison with DMSO control values.

implicated in the regulation of follicular development, with *Akt1* knockout mice displaying reduced fertility characterized by abnormal folliculogenesis and *Akt2* overexpression being associated with increased cell survival in the ovary (Brown *et al.*, 2010). *Akt1* has been shown to regulate folliculogenesis via the PI3K/Akt signaling pathway, which itself has been implicated in primordial follicle survival and activation (Reddy *et al.*, 2009).

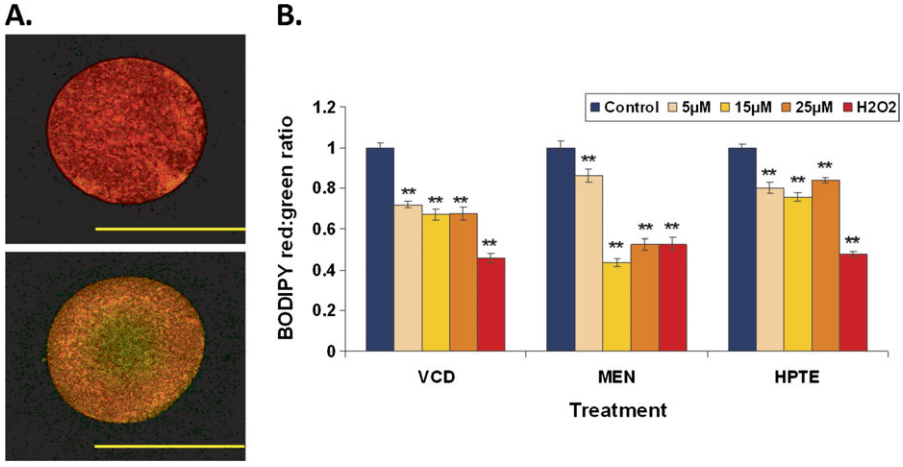

FIG. 7. Xenobiotic-induced oocyte membrane lipid peroxidation *in vitro*. Oocytes obtained from superovulated mice were cultured in a xenobiotic-treated medium for 2 h and labeled with BODIPY fluorescent dye as outlined in the Materials and Methods section. (A) Representative images of BODIPY-labeled DMSO-treated (top) and H_2O_2-treated (bottom) oocytes. Scale bar is equal to 100 µm. (B) Levels of lipid peroxidation as measured by the ratio of red:green fluorescence in varying concentrations of xenobiotics. Results were normalized to DMSO values for each experiment. H_2O_2 (8mM) was used as a representative of free radical ROS–induced lipid peroxidation. Values are mean ± SE, $n = 18–27$ oocytes from four mice. The symbols * and ** represent $p < 0.05$ and $p < 0.01$, respectively, in comparison with DMSO control values.

Another gene upregulated was *Sox4*, an important transcription factor of progenitor cell development and a regulator of the *Wnt* signaling pathway associated with follicular development (Boyer *et al*., 2009; Sinner *et al*., 2007). Interestingly, *Sox4* has also recently been found to transcriptionally activate growth factor receptors associated with PI3K/Akt signaling, making it a possible regulator of primordial follicle activation (Scharer *et al*., 2009). The identification of two members of the Akt family of protein kinases and a possible upstream regulator of the PI3K/Akt signaling pathway indicates an important mechanism of early preantral follicle ovotoxicity. In addition to genes associated with follicular development, VCD and MXC also upregulated the expression of *Mapk8*, and MAPK associated with induced atresia, and *Med1*, a DNA repair gene involved in p53-induced apoptosis (Frade *et al*., 2002; Hu *et al*., 2002).

Evidence of increased primordial follicle activation was found in VCD- and MXC-cultured ovaries by increased staining for PCNA in the granulosa cells and oocytes of primordial follicles (Chapman and Wolgemuth, 1994; Hutt *et al*., 2006). The markers of apoptosis, Casp2, Casp3, and TUNEL were all detected in small developing follicles from the primary stage onward. Studies involving mice deficient in Casp2 have identified the cysteine protease as a marker for cell death in the oocyte, whereas Casp3 is critical for granulosa cell apoptosis (Matikainen *et al*., 2001; Morita *et al*., 2001). Unfortunately, these results do not provide any insight into what cell type (granulosa cell or the oocyte) is targeted directly by VCD and MXC, as Casp2 and Casp3 were observed simultaneously in both primary and secondary follicles. The observed patterns of Casp2, Casp3, and TUNEL staining in VCD-treated ovaries have also been reported in similar studies using mice and rats, but the observed PCNA staining remains unique (Devine *et al*., 2002). Interestingly, these markers were not detected in the primordial follicles of VCD- and MXC-treated ovaries, indicating that these follicles were spared destruction.

Collectively, our results suggest a mechanism of VCD- and MXC-induced ovotoxicity involving small preantral follicular destruction and primordial follicle activation. The observed increase in primordial follicle activation may be because of a homeostatic mechanism of follicular replacement, maintaining the pool of developing follicles destroyed by xenobiotic exposure. Indeed, immunocontraception studies targeting zona proteins in developing follicles in the rabbit and marmoset primates are proposed to cause small preantral follicular destruction and primordial follicle activation through a similar mechanism (Paterson *et al*., 1992; Skinner *et al*., 1984). In further support for this hypothesis, *in vivo* experiments on xenobiotic-dosed neonatal mice also detected increased follicular activation and follicular depletion. This follicular replacement hypothesis has been previously suggested as a mode of VCD-induced primordial follicle depletion *in vitro*, but to our knowledge, this study is the first time that this hypothesis has been supported by microarray analysis and *in vivo* observations (Keating *et al*., 2009).

In addition to the follicular replacement hypothesis, follicle activation may be exacerbated by xenobiotic-induced oxidative stress. We have shown that xenobiotic exposure *in vitro* can cause oxidative stress and DNA damage, as evidenced by the detection of increased levels of 8-hydroxyguanine, a hydroxyl radical–induced DNA molecular lesion (Supplementary fig. 3) (Klaunig and Kamendulis, 2004). As recently reviewed by Wells *et al*. (2009), ROS play an important role in regulating signal transduction. Physiologically, ROS-mediated signal transduction occurs through H_2O_2, which selectively oxidizes cysteine residues on proteins resulting in a variety of reversible molecular interactions. We propose that increased levels of H_2O_2 caused by xenobiotic detoxification could lead to perturbed cysteine oxidation and upregulation of PI3K/Akt signaling through the inactivation of phosphatises, which negatively regulate the pathway via H_2O_2 oxidation (Kim *et al*., 2005; Naughton *et al*., 2009).

Unlike VCD and MXC, MEN upregulated pathways implicated in follicular atresia, the immune response, and xenobiotic metabolism. Although upregulation of apoptotic and xenobiotic-metabolizing pathways was expected, upregulation of immune response pathways such as the dendritic cell maturation pathway, the antigen presentation pathway, and interleukin-4 signaling was not. We propose that these pathways become activated because of oxidative stress following MEN quinone redox cycling (Cadenas and Davies, 2000; Kantengwa *et al*., 2003; Powis *et al*., 1981). MEN-induced ovotoxicity chiefly induces primordial and primary follicular atresia *in vitro* as indicated by increased Casp2 and Casp3 staining in developing follicles and widespread DNA damage in MEN-cultured neonatal ovaries (Fig. 3). Our *in vivo* follicular composition analysis of low-dose MEN supports these results; however, high-dose MEN *in vivo* analysis revealed increased follicular activation alongside increased small preantral follicular depletion. These results are intriguing and could be the result of differences between MEN metabolism in ovarian culture and *in vivo*. In the rodent liver, MEN is metabolized through a two-stage electron reduction into menadiol, which is then enzymatically conjugated to glucuronide and excreted from the body (Jarabak and Jarabak, 1995; Thompson *et al*., 1972). The resulting menadiol glucuronide conjugate is less reactive than MEN and therefore less toxic. The ovary is capable of limited detoxification, as xenobiotic detoxifying enzymes are increased (Supplementary fig. 2) (Cannady *et al*., 2003). However, as evidenced by the effect on follicular destruction in the low-dose treatments, it was still more potent than VCD and MXC.

Gamete interaction assays revealed severely reduced sperm-egg binding and fusion in a dose-dependent manner for all the xenobiotic treatments (Fig. 6). To our knowledge, this is the first evidence of short-term neonatal exposure to xenobiotics reducing fertilization at sexual maturity. Additionally, these results demonstrate that low-dose xenobiotic exposures, which do not profoundly affect the follicular population, can cause

oocyte dysfunction (Figs. 5 and 6). As sperm-egg fusion assays are an indicator of oocyte membrane fluidity, it was suggested that the reduced levels of sperm-egg binding and fusion were because of peroxidative damage to the oocyte plasma membrane. Oocyte lipid peroxidation is a physiological process that is thought to occur after the penetration of the membrane by an oxidizing spermatozoon, with the resulting change in plasma membrane fluidity acting as a block to polyspermy (Perry and Epel, 1985). We propose that xenobiotic-induced ROS initiate this process prematurely in the ovary, causing the observed impaired sperm-egg binding/fusion. To confirm xenobiotic exposure could lead to oocyte lipid peroxidation, levels of lipid peroxidation were measured in xenobiotic-cultured MII oocytes. All xenobiotics or their metabolites (Miller *et al*., 2006) induced lipid peroxidation (Diaz *et al*., 2007; Swain and Smith, 2007). These results support the view that xenobiotic exposure can cause oocyte dysfunction by altering the fluidity of the oocyte plasma membrane, thus impairing fertilization.

These findings challenge the established dogma of preantral ovotoxicity, which suggests that a xenobiotic is only harmful at concentrations where it induces follicular loss and that once it is removed from the immediate environment female fertility can revert to normal. Our data indicate that even a short-term, low-dose xenobiotic exposure that does not induce follicular atresia can cause lasting effects on oocyte quality in the form of xenobiotic ROS–induced oocyte dysfunction, even after it is removed from the environment. Additionally, these results also raise the possibility of using low-dose xenobiotic exposures to study the effects of mitochondrial loss in the ageing oocyte, a postulated cause of poor fertility in older women (Tarin, 1996)

In summary, our results support a mechanism of preantral ovotoxicity involving the homeostatic recruitment of primordial follicles to maintain the pool of developing follicles destroyed by xenobiotic exposure. These results also provide evidence of an overlapping mechanism of preantral ovotoxicity between VCD and MXC demonstrated by similarities in gene expression and affect on folliculogenesis *in vitro* and *in vivo*. To our knowledge, these studies also demonstrate for the first time that short-term xenobiotic exposure can cause long-term oocyte dysfunction, even at levels which do not have an adverse affect on follicular composition.

SUPPLEMENTARY DATA

Supplementary data are available online at http://toxsci.oxfordjournals.org/.

FUNDING

Australian Research Council; Hunter Medical Research Institute; Newcastle Permanent Building Society Charitable Trust to E.A.M.; National Health and Medical Research Council (Project grant #510735) to E.A.M., S.D.R., B.N.

ACKNOWLEDGMENTS

A.P.S. is the recipient of a Australian Postgraduate Award PhD scholarship. The authors would also like to thank Skye Courtney McIver for her technical assistance.

REFERENCES

Bayrak, A., and Oktay, K. (2003). The expression of cyclin-dependent kinase inhibitors p 15, p 16, p 21, and p 27 during ovarian follicle growth initiation in the mouse. *Reprod. Biol. Endocrinol.* **1,** 41.

Borgeest, C., Miller, K. P., Gupta, R., Greenfeld, C., Hruska, K. S., Hoyer, P., and Flaws, J. A. (2004). Methoxychlor-induced atresia in the mouse involves Bcl-2 family members, but not gonadotropins or estradiol. *Biol. Reprod.* **70,** 1828–1835.

Borgeest, C., Symonds, D., Mayer, L. P., Hoyer, P. B., and Flaws, J. A. (2002). Methoxychlor may cause ovarian follicular atresia and proliferation of the ovarian epithelium in the mouse. *Toxicol. Sci.* **68,** 473–478.

Borman, S. M., Christian, P. J., Sipes, I. G., and Hoyer, P. B. (2000). Ovotoxicity in female Fischer rats and B6 mice induced by low-dose exposure to three polycyclic aromatic hydrocarbons: comparison through calculation of an ovotoxic index. *Toxicol. Appl. Pharmacol.* **167,** 191–198.

Boyer, A., Goff, A. K., and Boerboom, D. (2009). WNT signaling in ovarian follicle biology and tumorigenesis. *Trends Endocrinol. Metab.* **21,** 25–32.

Brown, C., LaRocca, J., Pietruska, J., Ota, M., Anderson, L., Duncan Smith, S., Weston, P., Rasoulpour, T., and Hixon, M. L. (2010). Subfertility caused by altered follicular development and oocyte growth in female mice lacking PKBalpha/Akt1. *Biol. Reprod.* **82,** 246–256.

Cadenas, E., and Davies, K. J. A. (2000). Mitochondrial free radical generation, oxidative stress, and aging. *Free Radic. Biol. Med.* **29,** 222–230.

Cannady, E. A., Dyer, C. A., Christian, P. J., Sipes, I. G., and Hoyer, P. B. (2003). Expression and activity of cytochromes P450 2E1, 2A, and 2B in the mouse ovary: the effect of 4-vinylcyclohexene and its diepoxide metabolite. *Toxicol. Sci.* **73,** 423–430.

Chapman, D. L., and Wolgemuth, D. J. (1994). Expression of proliferating cell nuclear antigen in the mouse germ line and surrounding somatic cells suggests both proliferation-dependent and -independent modes of function. *Int. J. Dev. Biol.* **38,** 491–497.

Chomczynski, P., and Sacchi, N. (1987). Single-step method of RNA isolation by acid guanidinium thiocyanate-phenol-chloroform. *Anal. Biochem.* **162,** 156–159.

Danielson, P. B. (2002). The cytochrome P450 superfamily: biochemistry, evolution and drug metabolism in humans. *Curr. Drug Metab.* **3,** 561–597.

Datta, S. R., Brunet, A., and Greenberg, M. E. (1999). Cellular survival: a play in three Akts. *Genes Dev.* **13,** 2905–2927.

Devine, P. J., Sipes, I. G., Skinner, M. K., and Hoyer, P. B. (2002). Characterization of a rat in vitro ovarian culture system to study the ovarian toxicant 4-vinylcyclohexene diepoxide. *Toxicol. Appl. Pharmacol.* **184,** 107–115.

Diaz, F. J., Wigglesworth, K., and Eppig, J. J. (2007). Oocytes are required for the preantral granulosa cell to cumulus cell transition in mice. *Dev. Biol.* **305,** 300–311.

Frade, R., Balbo, M., and Barel, M. (2002). RB18A regulates p53-dependent apoptosis. *Oncogene* **21,** 861–866.

Gupta, R. K., Meachum, S., Hernández-Ochoa, I., Peretz, J., Yao, H. H., and Flaws, J. A. (2009). Methoxychlor inhibits growth of antral follicles by altering cell cycle regulators. *Toxicol. Appl. Pharmacol.* **240,** 1–7.

Gupta, R. K., Schuh, R. A., Fiskum, G., and Flaws, J. A. (2006). Methoxychlor causes mitochondrial dysfunction and oxidative damage in the mouse ovary. *Toxicol. Appl. Pharmacol.* **216,** 436–445.

Hirshfield, A. N. (1991). Development of follicles in the mammalian ovary. *Int. Rev. Cytol. Surv. Cell Biol.* **124,** 43–101.

Holt, J. E., Jackson, A., Roman, S. D., Aitken, R. J., Koopman, P., and McLaughlin, E. A. (2006). CXCR4/SDF1 interaction inhibits the primordial to primary follicle transition in the neonatal mouse ovary. *Dev. Biol.* **293,** 449–460.

Hoyer, P. B., and Sipes, I. G. (1996). Assessment of follicle destruction in chemical-induced ovarian toxicity. *Annu. Rev. Pharmacol. Toxicol.* **36,** 307–331.

Hu, X., Christian, P., Sipes, I. G., and Hoyer, P. B. (2001). Expression and redistribution of cellular Bad, Bax, and Bcl-xL protein is associated with VCD-induced ovotoxicity in rats. *Biol. Reprod.* **65,** 1489–1495.

Hu, X., Flaws, J. A., Sipes, I. G., and Hoyer, P. B. (2002). Activation of mitogen-activated protein kinases and AP-1 transcription factor in ovotoxicity induced by 4-vinylcyclohexene diepoxide in rats. *Biol. Reprod.* **67,** 718–724.

Hu, X., Roberts, J. R., Apopa, P. L., Kan, Y. W., and Ma, Q. (2006). Accelerated ovarian failure induced by 4-vinyl cyclohexene diepoxide in Nrf2 null mice. *Mol. Cell. Biol.* **26,** 940–954.

Huang, J. H. Y., Rajkovic, A., Szafranski, P., Ochsner, S., Richards, J. A., and Goode, S. (2003). Expression of Drosophila neoplastic tumor suppressor genes discslarge, scribble, and lethal giant larvae in the mammalian ovary. *Gene Expr. Patterns.* **3,** 3–11.

Hutt, K. J., McLaughlin, E. A., and Holland, M. K. (2006). Primordial follicle activation and follicular development in the juvenile rabbit ovary. *Cell Tissue Res.* **326,** 809–822.

Jarabak, R., and Jarabak, J. (1995). Effect of ascorbate on the DT-diaphorase-mediated redox cycling of 2-methyl-1, 4-naphthoquinone. *Arch. Biochem. Biophys.* **318,** 418–423.

Kantengwa, S., Jornot, L., Devenoges, C., and Nicod, L. P. (2003). Superoxide anions induce the maturation of human dendritic cells. *Am. J. Respir. Critic. Care Med.* **167,** 431–437.

Kao, S. W., Sipes, I. G., and Hoyer, P. B. (1999). Early effects of ovotoxicity induced by 4-vinylcyclohexene diepoxide in rats and mice. *Reprod. Toxicol.* **13,** 67–75.

Kascheike, B., and Walther, N. (1997). Alterations in the chromatin structure of the distal promoter region of the bovine oxytocin gene correlate with ovarian expression. *DNA Cell Biol.* **16,** 1237–1248.

Keating, A. F., Mark, C. J., Sen, N., Sipes, I. G., and Hoyer, P. B. (2009). Effect of phosphatidylinositol-3 kinase inhibition on ovotoxicity caused by 4-vinylcyclohexene diepoxide and 7, 12-dimethylbenz [a] anthracene in neonatal rat ovaries. *Toxicol. Appl. Pharmacol.* **241,** 127–134.

Kim, J. H., Chu, S. C., Gramlich, J. L., Pride, Y. B., Babendreier, E., Chauhan, D., Salgia, R., Podar, K., Griffin, J. D., and Sattler, M. (2005). Activation of the PI3K/mTOR pathway by BCR-ABL contributes to increased production of reactive oxygen species. *Blood* **105,** 1717–1723.

Klaunig, J. E., and Kamendulis, L. M. (2004). The role of oxidative stress in carcinogenesis. *Annu. Rev. Pharmacol. Toxicol.* **44,** 239–267.

Matikainen, T., Perez, G. I., Zheng, T. S., Kluzak, T. R., Rueda, B. R., Flavell, R. A., and Tilly, J. L. (2001). Caspase-3 gene knockout defines cell lineage specificity for programmed cell death signaling in the ovary. *Endocrinology* **142,** 2468–2480.

McGee, E. A., and Hsueh, A. J. W. (2000). Initial and cyclic recruitment of ovarian follicles. *Endocr. Rev.* **21,** 200–214.

McLaughlin, E. A., and McIver, S. C. (2009). Awakening the oocyte: controlling primordial follicle development. *Reproduction* **137,** 1–11.

Miller, K. P., Gupta, R. K., and Flaws, J. A. (2006). Methoxychlor metabolites may cause ovarian toxicity through estrogen-regulated pathways. *Toxicol. Sci.* **93,** 180–188.

Morita, Y., Maravei, D. V., Bergeron, L., Wang, S., Perez, G. I., Tsutsumi, O., Taketani, Y., Asano, M., Horai, R., and Korsmeyer, S. J. (2001). Caspase-2 deficiency rescues female germ cells from death due to cytokine insufficiency but not meiotic defects caused by ataxia telangiectasia-mutated (Atm) gene inactivation. *Cell Death Differ.* **8,** 614–620.

Muñiz, L. C., Yehia, G., Mémin, E., Ratnakar, P., and Molina, C. A. (2006). Transcriptional regulation of cyclin D2 by the PKA pathway and inducible cAMP early repressor in granulosa cells. *Biol. Reprod.* **75,** 279–288.

Naughton, R., Quiney, C., Turner, S. D., and Cotter, T. G. (2009). Bcr-Abl-mediated redox regulation of the PI3K/AKT pathway. *Leukemia* **23,** 1432–1440.

Neal, M. S., Zhu, J., Holloway, A. C., and Foster, W. G. (2007). Follicle growth is inhibited by benzo-[a]-pyrene, at concentrations representative of human exposure, in an isolated rat follicle culture assay. *Hum. Reprod.* **22,** 961–967.

Paterson, M., Koothan, P. T., Morris, K. D., O'Byrne, K. T., Braude, P., Williams, A., and Aitken, R. J. (1992). Analysis of the contraceptive potential of antibodies against native and deglycosylated porcine ZP3 in vivo and in vitro. *Biol. Reprod.* **46,** 523–534.

Perry, G., and Epel, D. (1985). Fertilization stimulates lipid peroxidation in the sea urchin egg* 1. *Dev. Biol.* **107,** 58–65.

Powis, G., Svingen, B. A., and Appel, P. (1981). Quinone-stimulated superoxide formation by subcellular fractions, isolated hepatocytes, and other cells. *Mol. Pharmacol.* **20,** 387–394.

Radjendirane, V., Joseph, P., Lee, Y. H., Kimura, S., Klein-Szanto, A. J. P., Gonzalez, F. J., and Jaiswal, A. K. (1998). Disruption of the DT diaphorase (NQO1) gene in mice leads to increased menadione toxicity. *J. Biol. Chem.* **273,** 7382–7389.

Reddy, P., Adhikari, D., Zheng, W., Liang, S., Hamalainen, T., Tohonen, V., Ogawa, W., Noda, T., Volarevic, S., and Huhtaniemi, I. (2009). PDK1 signaling in oocytes controls reproductive aging and lifespan by manipulating the survival of primordial follicles. *Hum. Mol. Genet.* **18,** 2813–2824.

Rucker, E. B., III., Dierisseau, P., Wagner, K. U., Garrett, L., Wynshaw-Boris, A., Flaws, J. A., and Hennighausen, L. (2000). Bcl-x and Bax regulate mouse primordial germ cell survival and apoptosis during embryogenesis. *Mol. Endocrinol.* **14,** 1038–1052.

Scharer, C. D., McCabe, C. D., Ali-Seyed, M., Berger, M. F., Bulyk, M. L., and Moreno, C. S. (2009). Genome-wide promoter analysis of the SOX4 transcriptional network in prostate cancer cells. *Cancer Res.* **69,** 709–717.

Sinner, D., Kordich, J. J., Spence, J. R., Opoka, R., Rankin, S., Lin, S. C. J., Jonatan, D., Zorn, A. M., and Wells, J. M. (2007). Sox17 and Sox4 differentially regulate {beta}-catenin/T-cell factor activity and proliferation of colon carcinoma cells. *Mol. Cell. Biol.* **27,** 7802–7815.

Skinner, S. M., Mills, T., Kirchick, H. J., and Dunbar, B. S. (1984). Immunization with zona pellucida proteins results in abnormal ovarian follicular differentiation and inhibition of gonadotropin-induced steroid secretion. *Endocrinology* **115,** 2418–2432.

Swain, J. E., and Smith, G. D. (2007). Reversible phosphorylation and regulation of mammalian oocyte meiotic chromatin remodeling and segregation. *Soc. Reprod. Fertil. Suppl.* **63,** 343–358.

Tarin, J. J. (1996). Potential effects of age-associated oxidative stress on mammalian oocytes/embryos. *Mol. Hum. Reprod.* **2,** 717–724.

Thompson, R. M., Gerber, N., Seibert, R. A., and Desiderio, D. M. (1972). Identification of 2-methyl-1, 4-naphthohydroguinone monoglucuronide as a metabolite of 2-methyl-1, 4-naphthoquinone (menadione) in rat bile. *Res. Commun. Chem. Pathol. Pharmacol.* **4,** 543–552.

Wells, P. G., McCallum, G. P., Chen, C. S., Henderson, J. T., Lee, C. J. J., Perstin, J., Preston, T. J., Wiley, M. J., and Wong, A. W. (2009). Oxidative stress in developmental origins of disease: teratogenesis, neurodevelopmental deficits, and cancer. *Toxicol. Sci.* **108,** 4–18.

Xing, W., and Sairam, M. R. (2002). Retinoic acid mediates transcriptional repression of ovine follicle-stimulating hormone receptor gene via a pleiotropic nuclear receptor response element. *Biol. Reprod.* **67,** 204–211.